Supporting Information

Tunable Color-Stable Hybrid White OLEDs by Combining Fluorescent and TADF Emitters in a Single Emissive Layer

*Upasana Deori, Thamodharan Viswanathan, Nisha Yadav, Pachaiyappan Rajamalli**

Materials Research Centre, Indian Institute of Science, Bangalore – 560012, Karnataka, India.

*E-mail: rajamalli@iisc.ac.in

Contents

1. General Information

1.1 Instrumentation

The ^{1}H (400 MHz) and ^{13}C NMR (100 MHz) characterization were performed using Bruker Advance 400 spectrometer. The HRMS were measured using MAT-95XL HRMS. The ultraviolet-visible (UV-Vis) absorption spectra were taken from the Jasco *V*-730 spectrophotometer. The photoluminescence (PL) spectra in both solutions and films were obtained using Hitachi F-7100 fluorescence spectrophotometer. The time-resolved photoluminescence decay (TRPL) spectra of the films were recorded with Edinburgh FLS1000 spectrometer coupled with a double monochromator for both excitation and emission. The thermal stability of the anthracene emitter was studied using Q50 TGA thermogravimetric analyzer. The cyclic voltammetry measurement was carried out in deoxygenated dichloromethane (DCM) with 0.1 M tetrabutylammonium hexafluorophosphate (TBAP) as supporting electrolyte in a three-electrode system using BioLogic SP50 potentiostat. The counter, working and reference electrodes were platinum wire, glassy carbon, and Ag/AgCl/KCl (saturated), respectively. The HOMO energy levels were determined from the onset of the oxidation potential using the equation – (4.8 eV + E_{ox} (vs Fc_{ox})), while the LUMO energy levels were calculated from the optical band gap (E_g) and the HOMO levels.

1.2 Device fabrication

The OLEDs were fabricated using a vacuum deposition technique on indium-tin-oxide (ITO) coated glass substrates, which behave as an anode. The ITO surfaces were cleaned ultrasonically with deionized water, acetone, and isopropanol. The substrates were dried with N_2 blow and exposed to ultraviolet (UV) light and ozone treatment for 20 mins to improve hole injection, before loading them in a high vacuum chamber (10^{-6} torr) for thermal evaporation. The organic layers were deposited onto the substrates at a rate of 1.0 Å s^{-1}, followed by Liq

and Al with rates 0.1 Å s^{-1} and 3-7 Å s^{-1}, respectively. The OLED devices' active area was 4.5 mm^2. The electroluminance measurements were performed at ambient conditions using a Keithley 2450 source meter, which is connected to a silicon photodetector. The external quantum efficiency (EQE) values were calculated from the electroluminance spectra, assuming the Lambertian emission profile.

2. Experimental Section

Synthesis and characterization

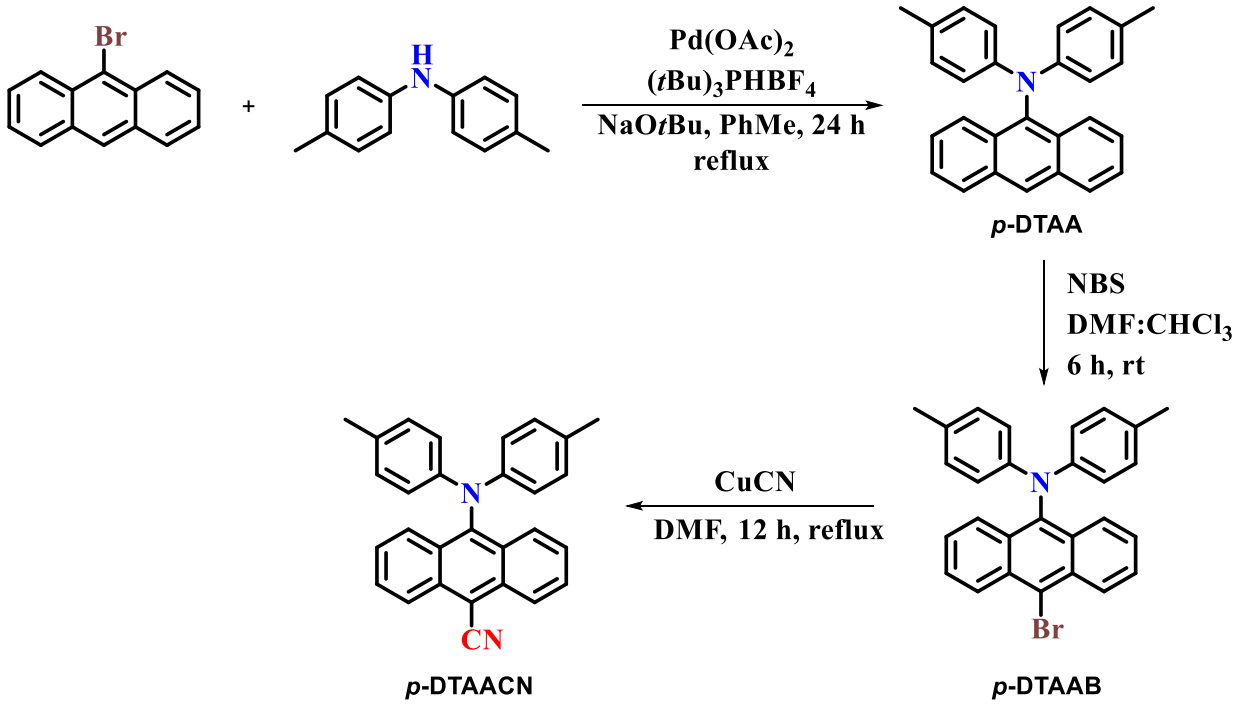

Scheme S1. Synthetic route for the fluorescent emitter.

Synthesis of *p*-ditolylanthracen-9-amine (*p*-DTAA)

A mixture of 9-bromoanthracene (5.00 g, 19.6 mmol), $Pd(OAc)_2$ (220.0 mg, 0.98 mmol), tri-*tert*-butylphosphine (853.0 mg, 2.94 mmol), di-*p*-tolylamine (4.24 g, 21.6 mmol) and sodium *tert*-butoxide (3.77 g, 39.2 mmol) in dry *o*-xylene (40 mL) was placed in a sealed tube under a nitrogen atmosphere and was stirred at 120 °C for 15 h. After cooling, water was added to the reaction mixture and the mixture was then extracted with ethyl acetate. The organic layer

was dried over anhydrous $MgSO_4$ and evaporated under vacuum. The crude product was purified by silica gel column chromatography eluted with *n*-hexane to give the desired yellow solid in 68% yield.[1]

Synthesis of *p*- ditolylamino anthracenebromide (*p*-D**TAAB**)

***p*-DTAA** (3.5 g, 9.3 mmol) and *N*-bromosuccinimide (NBS) (1.66 g, 9.3 mmol) were dissolved in DMF : $CHCl_3$ (1 : 3, 50 mL) and the solution was stirred at room temperature for 6 h. After completion of reaction, water was added to the reaction mixture and the mixture was extracted with dichloromethane. The organic layer was dried over anhydrous $MgSO_4$ and evaporated under vacuum. The product was purified by silica gel column chromatography eluted with *n*-hexane. Red crystals of **TAAB** were obtained in 70% yield.[1]

Synthesis of *p*-ditolylamino anthracene carbonitrile *p*-DTAACN

***p*-DTAAB** (3 g, 6.65 mmol) and 890 mg (9.98 mmol) of CuCN were combined in a round bottom flask with 20 mL of DMF. The mixture was put under N_2 and refluxed for 12 hours and cooled to room temperature. The DMF was distilled off under vacuum and crude solid was purified by silica gel column chromatography using ethyl acetate/hexane as the eluent. The product ***p*-DTAACN** is red solid and were obtained in 64% yield.

^{1}H NMR (400 MHz, $CDCl_3$): δ = 8.41 (d, 2H, J = 8.8 Hz), 8.38 (d, 2H, J = 8.8 Hz), 7.60 (m, 2H), 7.39 (m, 2H), 6.91 (d, 4H, J = 8.0 Hz), 6.83 (d, 4H, J = 8.4 Hz), 6.56 (q, 1H, J = 1.6 Hz), 1.39 (s, 36H). ^{13}C NMR (100 MHz, $CDCl_3$): δ = 145.4, 143.9, 134.7, 131.3, 130.1, 130.0, 128.8, 127.3, 126.0, 125.5, 120.5, 117.4, 105.0, 20.6. HRMS (ESI-TOF) m/z: $[M]^+$ Calculated for $C_{29}H_{22}N_2$ 398.1783; Found 398.1780.

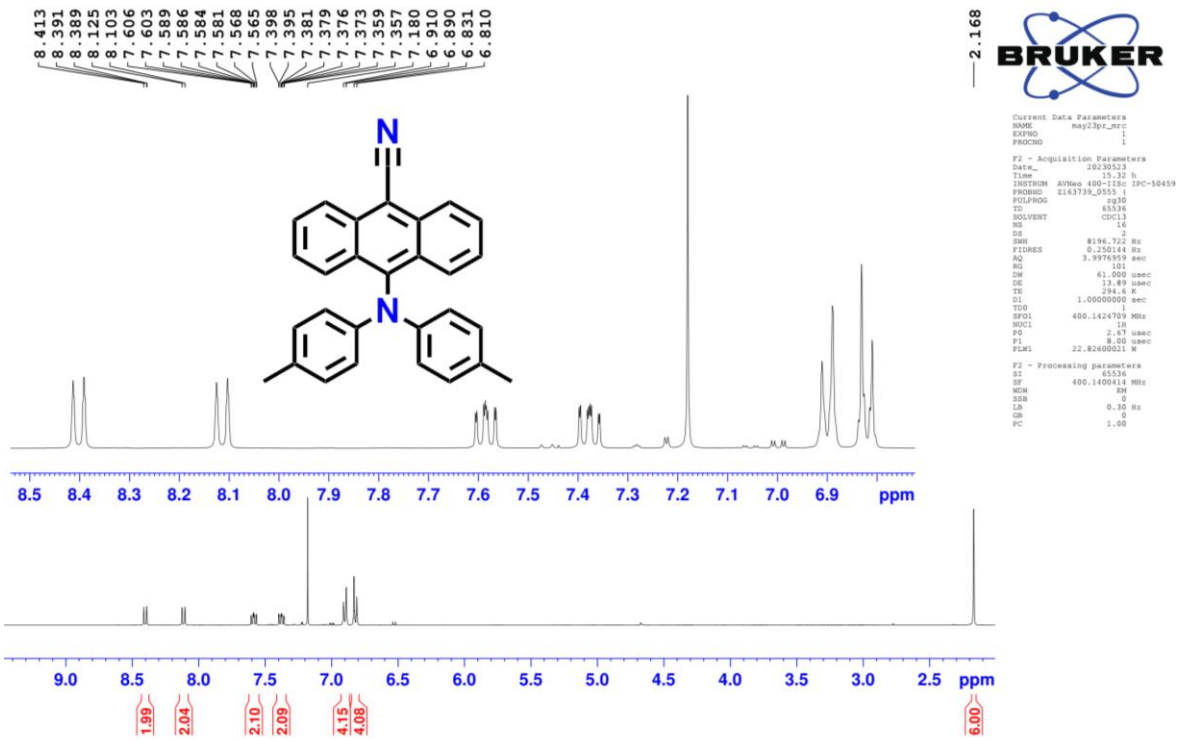

Fig. S1 ^{1}H NMR of ***p*-DTAACN** in $CDCl_3$.

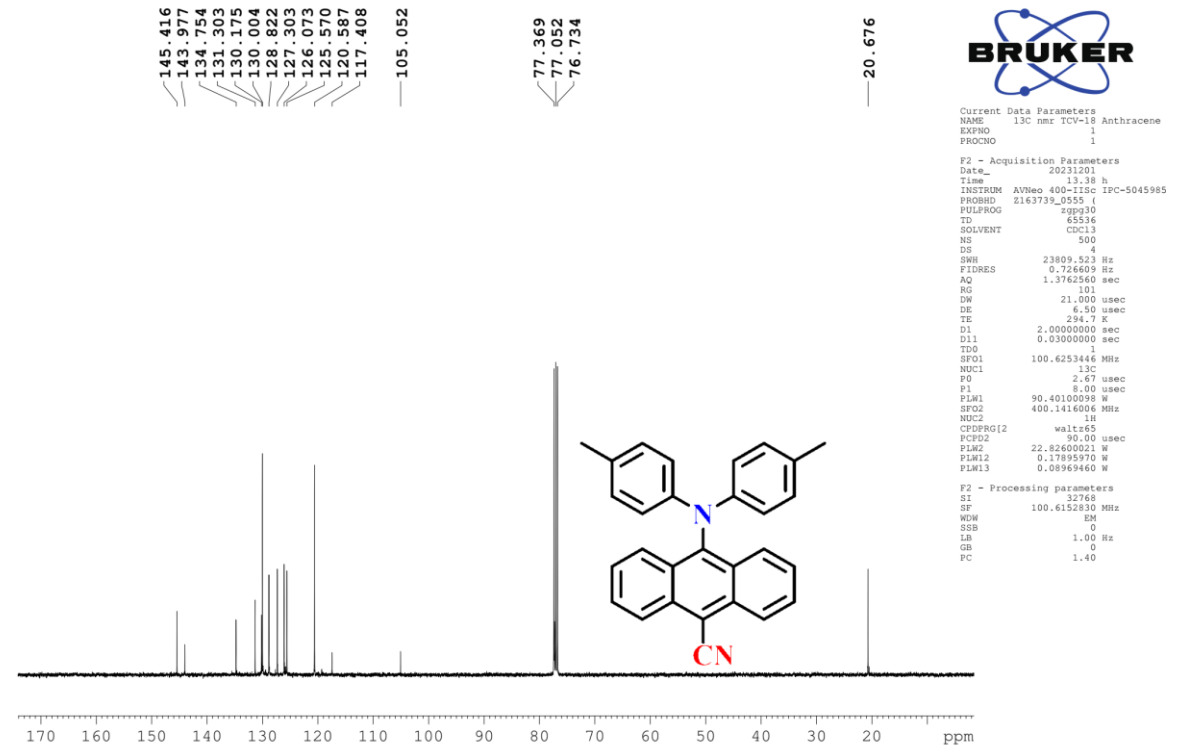

Fig. S2 ^{13}C NMR of ***p*-DTAACN** in $CDCl_3$.

3. XRD

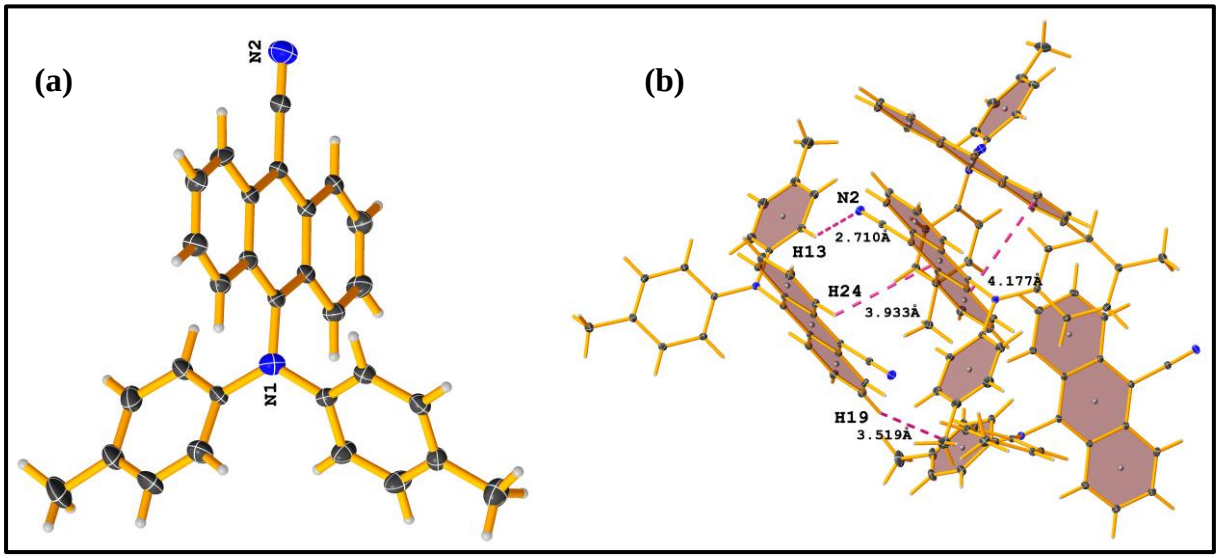

Fig. S3 (a) Single-crystal structure and (b) non-covalent interaction in the packing of *p*-DTAACN.

4. Thermal stability

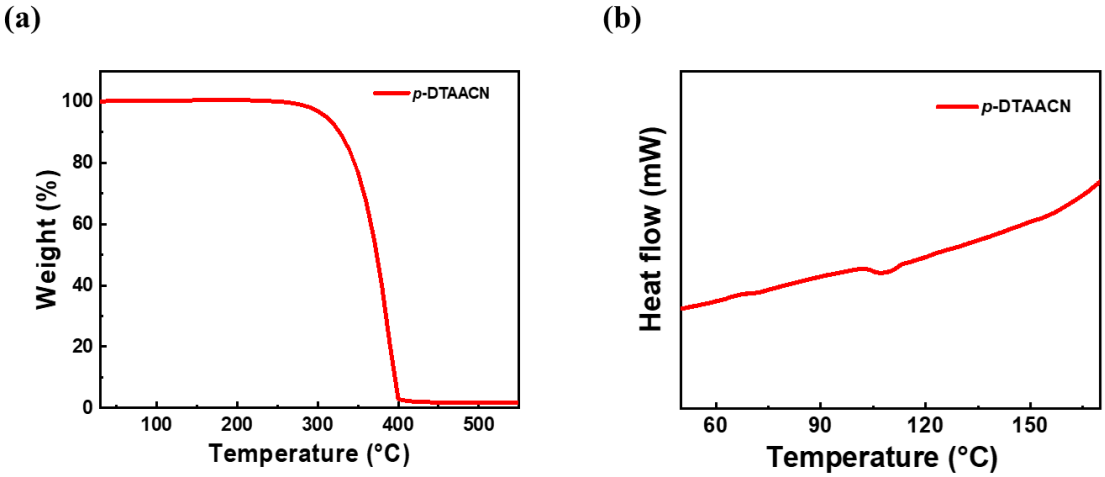

Fig. S4 (a)Thermogravimetric analysis (TGA) and (b) Differential scanning calorimetry (DSC) plot of *p*-DTAACN

5. Solvatochromic study

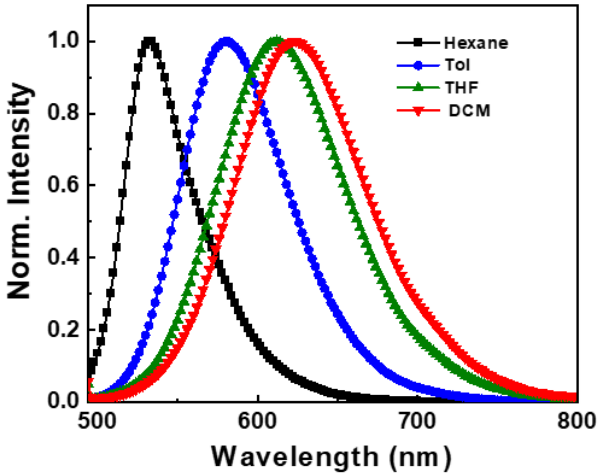

Fig. S5 Solvatochromic study for *p*-DTAACN in solution (10^{-5} M).

6. Cyclic Voltammetry

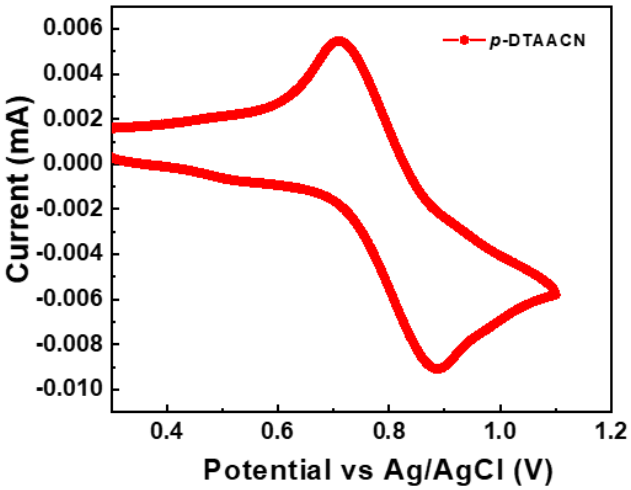

Fig. S6 Cyclic voltammogram of *p*-DTAACN in dry dichloromethane (DCM) (1 mM solution) using 0.1 M tetrabutylammonium hexafluorophosphate (TBAP) as supporting electrolyte and glassy carbon as the working electrode and Ag/AgCl/KCl (sat.) as a reference electrode.

7. Device structure and EL spectra of *p*-DTAACN

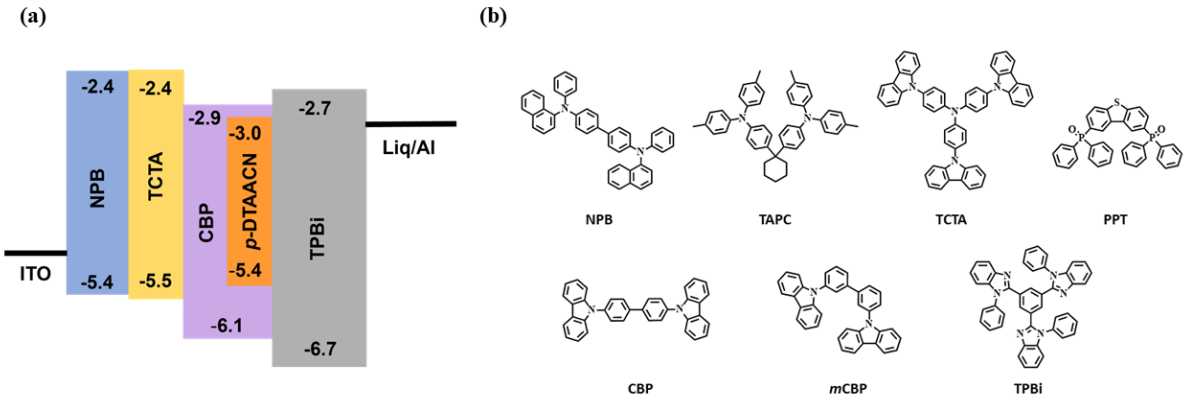

Fig. S7 (a) Energy level diagram of the optimized *p*-DTAACN device structure. (b) Molecular structures of different materials used in the device structure.

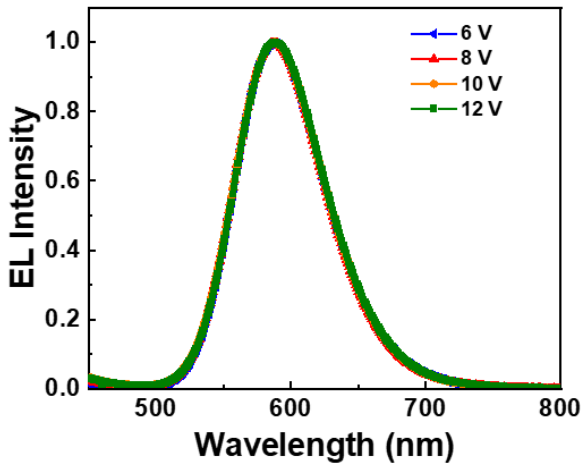

Fig. S8 Electroluminescence spectra of *p*-DTAACN device at various operating voltages.

8. Photophysical study of 3BPy-*m*DTC and *p*-DTAACN

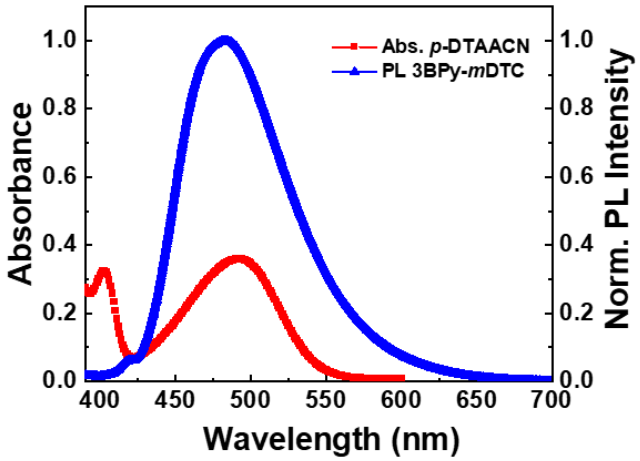

Fig. S9 The absorption spectra of *p*-DTAACN and photoluminescence emission spectra of 3BPy-*m*DTC in toluene solutions with 10^{-5} M concentration[2-4].

9. Device characteristics of WOLEDs

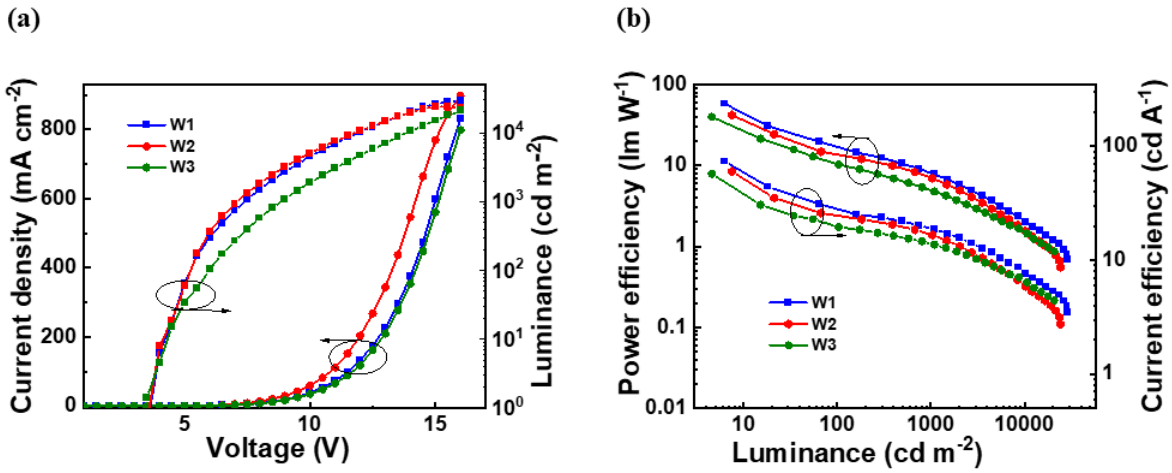

Fig. S10 (a) Current density-voltage-luminance (*J*-*V*-*L*) curves, (b) Power efficiency-Luminance-Current efficiency characteristics of the WOLEDs, W1-W3.

10. Transient Photoluminescence decay

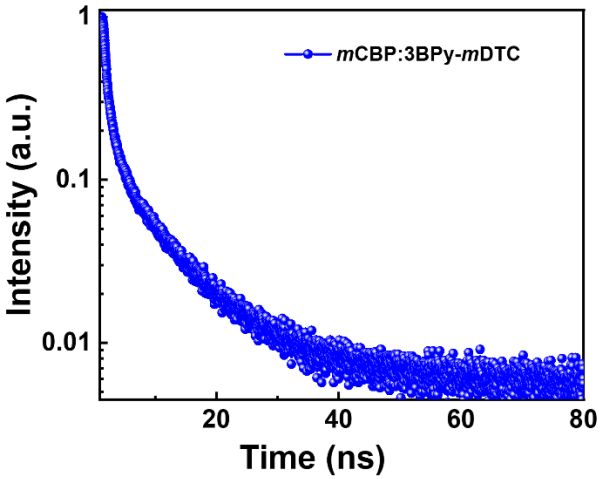

Fig. S11 Prompt PL decay curve of *m*CBP:3BPy-*m*DTC film, with excitation wavelength 340 nm and emission wavelength 479 nm.

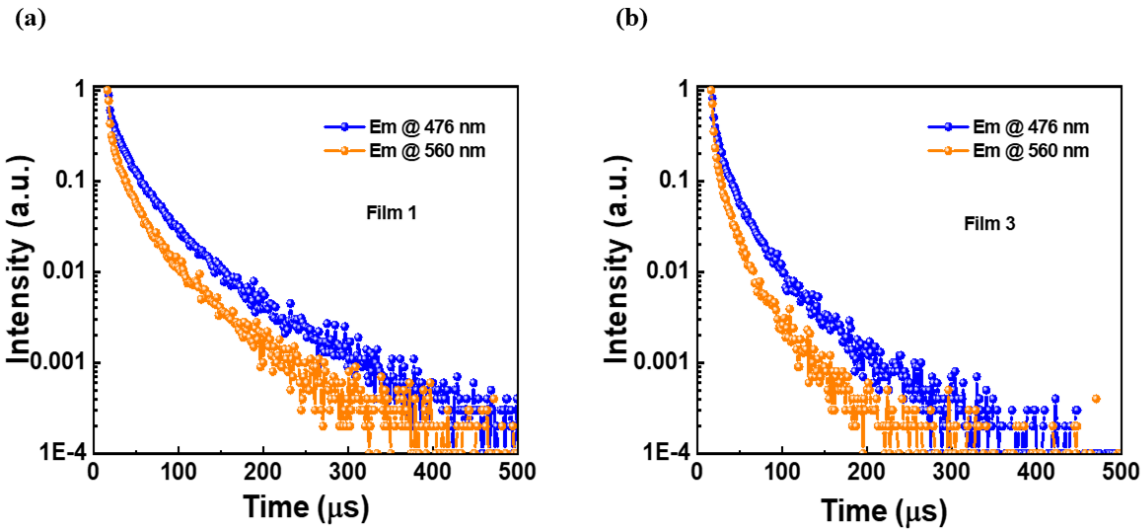

Fig. S12 Transient photoluminescence decay curves of doped white films, (a) film 1 (0.5 wt.% *p*-DTAACN and (b) film 3 (1.0 wt.% *p*-DTAACN), observed at the PL emission peaks of 476 nm and 560 nm and excitation of 340 nm.

11. Reference

1. P. Rajamalli, P. Gandeepan, M. J. Huang and C. H. Cheng, *J. Mater. Chem. C*, 2015, **3**, 3329–3335.
2. P. Rajamalli, V. Thangaraji, N. Senthilkumar, C. C. Ren-Wu, H. W. Lin and C. H. Cheng, *J. Mater. Chem. C*, 2017, **5**, 2919–2926.
3. K. Gao, K. Liu, X. L. Li, X. Cai, D. Chen, Z. Xu, Z. He, B. Li, Z. Qiao, D. Chen, Y. Cao and S. J. Su, *J. Mater. Chem. C*, 2017, **5**, 10406–10416.
4. H. Liu, J. Chen, Y. Fu, Z. Zhao and B. Z. Tang, *Adv. Funct. Mater.*, 2021, **31**, 2103273.